Heliyon 10 (2024) e37084

Contents lists available at ScienceDirect

Heliyon

journal homepage: www.cell.com/heliyon

Research article

# Experimental analysis of the cyclic behavior of rammed earth walls reinforced with arundo donax natural fiber

Viviana Mora-Ruiz [a,*], Cristian Mejía-Parada [a], Brayam Nuñez [b], Sergio M. Pineda [c], Néstor I. Prado [c], Jose Agustin Vallejo-Borda [a,d], Jair Arrieta-Baldovino [e]

[a] *Universidad de Investigación y Desarrollo, Facultad de Ingeniería Civil, Grupo de Investigación en Amenazas, Vulnerabilidad y Riesgos a Fenómenos Naturales, Cl. 9 # 23-55, 680001, Bucaramanga, Santander, Colombia*

[b] *Universidad Pontificia Bolivariana, Facultad de Ingeniería Civil, Autopista Piedecuesta Kilómetro 7, Floridablanca, Santander, Colombia*

[c] *Universidad Pontificia Bolivariana, Facultad de Ingeniería Civil, Grupo de Investigación GRINDIC, Autopista Piedecuesta Kilómetro 7, Floridablanca, Santander, Colombia*

[d] *Departamento de Tecnologías Sostenibles y Civil, Tecnológico de Monterrey, Monterrey, Nuevo León, Mexico*

[e] *Universidad de Cartagena, Facultad de Ingeniería, Programa de Ingeniería Civil, Avenida Del Consulado Calle 30, 48-152, 130015, Cartagena de Indias, Colombia*

A R T I C L E I N F O

*Keywords:*
Rammed earth
Arundo donax natural fiber
Cyclic testing
Push and pull tests

A B S T R A C T

This experimental study analyzes the seismic behavior of rammed earth walls with Arundo donax natural fiber inclusions, also called "caña brava" (REWC), and without inclusions (REW). The experimental program consists of two stages: physical and mechanical characterization of materials, where properties such as particle size, density, Atterberg limits, and compressive and flexural strength were determined; and dynamic tests, which included compressive and cyclic load tests on REW and REWC walls. The walls were subjected to cyclic loading with derivatives between 0.2 % and 1.4 % in-plane combined with a constant vertical compressive stress of 13 kPa to simulate seismic forces in the presence of gravity loads. The results regarding loading, hysteretic response, energy dissipation, stiffness degradation, and failure mode are compared. In addition, the envelope curves of the load-displacement hysteretic responses are analyzed using a capacity spectrum approach. It is observed that the inclusion of Arundo donax natural fiber negatively affects the mechanical properties of the walls and their hysteretic response. It is also observed that the energy dissipation is affected by the inclusion of Arundo donax natural fiber. However, the stiffness behavior is similar in all the walls. Rigid body failure modes are identified in all the walls, but the walls, including Arundo donax natural fiber, form failure planes that divide the wall into two bodies.

## 1. Introduction

The production of conventional building materials requires 30–40 % of the total world energy, which has a negative impact on the environment [1]. Using locally available materials and improving traditional techniques is essential to promote sustainable

* Corresponding author.
*E-mail addresses:* jmora13@udi.edu.co (V. Mora-Ruiz), cmejia5@udi.edu.co (C. Mejía-Parada), nunez.romero@outlook.com (B. Nuñez), sergio.pineda@upb.edu.co (S.M. Pineda), nestor.prado@upb.edu.co (N.I. Prado), josevallejo@tec.mx (J.A. Vallejo-Borda), jarrietab2@unicartagena.edu.co (J. Arrieta-Baldovino).

https://doi.org/10.1016/j.heliyon.2024.e37084
Received 9 May 2024; Received in revised form 23 August 2024; Accepted 27 August 2024
Available online 28 August 2024

development. The rammed earth wall (REW) method is an ancestral technique used to compact wet soil in layers of 15–20 cm thickness in a wooden formwork [2,3]. Originating in Europe, this method spread throughout the American continent during the colonial era; however, during the 19th century, it declined due to using new materials such as cement. It has now re-emerged due to its sustainability, low cost, and ability to regulate temperature [4]. To construct these walls, a soil with a specific composition composed of 10–40 % clay, 10–40 % silt, and 35–65 % sand and fine gravel is required [2,3].

In the last decade, the use of various additives in the construction of rammed earth walls has been investigated. Among the most studied cementing agents are cement [5], lime [6], limestone [7], and blast furnace slag [8]. These cementitious agents bind particles and provide cohesion to construction mixtures, thus improving the strength and durability of the constructed elements.

On the other hand, in recent years, research has also been carried out into the incorporation of fibers in the construction of footing walling, using materials such as textiles [9], jute [10], coconut [10], wool [11], polypropylene fibers and steel [12]. These materials are integrated into rammed earth walls to improve their flexural strength and durability, which is crucial for strengthening earth structures and increasing their resistance to seismic loads.

The study of REW walls has mainly focused on mechanical behavior, emphasizing strength and durability [13]. In addition, thermal studies have been initiated to analyze the responses to temperature changes and the energy efficiency of these materials [11].

In developing countries, research has focused on how non-additive reinforced rammed earth walls (REW) respond to seismic motions, using mathematical models to predict structural responses [14]. Although some studies have employed simplified methods with static equivalents to evaluate the seismic response of REW [15], dynamic and pseudo-static methods are more accurate in simulating actual earthquake conditions [16]. However, the ancestral techniques of constructing rammed earth walls with the horizontal inclusion of Arundo donax have been little studied.

This research is focused on analyzing the construction technique of rammed earth walls with the inclusion of Arundo donax natural fiber (REWC) used in the department of Santander, Colombia. This technique is currently used in areas of medium-high seismic risk, including historic centers. However, no standards or guidelines exist to evaluate the mechanical and dynamic behavior of new earth constructions under cyclic loading in the region.

This experimental study analyzes the seismic behavior of rammed earth walls with Arundo donax natural fiber inclusions (REWC) and without inclusions (REW). The behavior of the walls was evaluated under cyclic loads with derivatives between 0.2 % and 1.4 %, combined with a constant vertical compressive stress of 13 kPa, which simulates the load of a housing roof. The research makes three contributions to the scientific community. First, a physical and mechanical analysis of the sustainable and traditional material, including the soil and the natural fiber of Arundo donax, is carried out. Secondly, a study of the structural behavior of the REW and REWC under cyclic loads that simulate the high seismic risk is analyzed. Thirdly, in the absence of specific regulations for new construction and detailed studies on the seismic behavior of REWC walls under cyclic loading in the study region. This research provides crucial data to indicate the risk of implementing the REWC technique and possible improvements to develop safer and sustainable earth construction buildings.

## 2. Experimental program

### 2.1. Materials and methods

The study's objective is to investigate the effect of including Arundo donax natural fiber on the cyclic resistance of the rammed earth walls. REW construction uses sustainable local materials; however, proper particle distribution and density of the compacted material are important. The choice of material is crucial for durability, compaction, and strength. Proper particle distribution is based on a balanced ratio of 10–40 % clay, 10–40 % silt, 35–65 % sand, and 10–20 % fine gravel, as recommended in sources [17]. The balanced ratio is crucial to balance fine, medium, and coarse particles, as fine particles provide cohesion and coarse particles provide

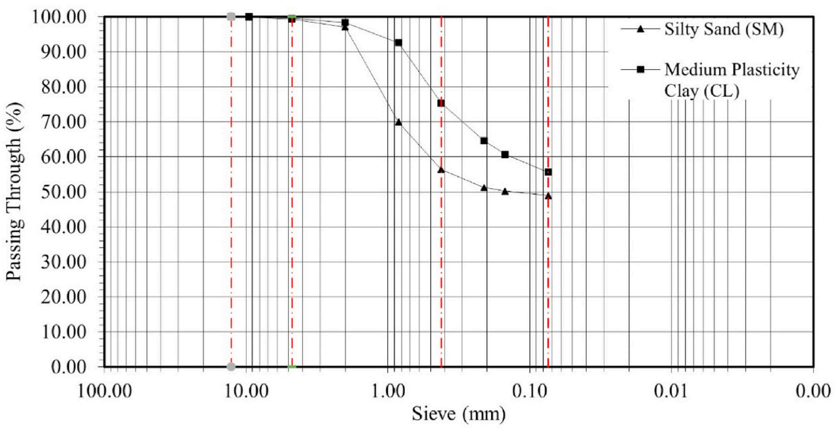


**Fig. 1.** Soil granulometric curve.

stability and strength [18].

Fig. 1 shows the grain size distribution of two materials considered for REW construction, classified according to the SUCS system based on their size, liquid limit, and plastic limit. One soil is identified as silty sand (SM), while the other is low-plasticity clay (CL).

Table 1 shows the percentages of each soil's liquid limit, plastic limit, plasticity index, fines content, sands, and gravels. Low-plasticity clayey soil was preferred for the walls because of its higher gradation and higher fine particle content. A medium to high clay content is beneficial for the cohesion of the sand particles without causing excessive shrinkage during drying, thus improving the strength and water-holding capacity of the material [19]. In addition, previous research suggests that a medium sand content increases soil durability, permeability, and density [20].

The Proctor test determined the maximum dry density and optimum soil moisture, obtaining values of 1.78 g/cm$^3$ and 18 %, respectively. These results are consistent with previous research on earthen walls. For example, in Iran, a moisture content between 14.61 % and 20.67 % was obtained, with maximum dry densities between 1.65 g/cm$^3$ and 1.79 g/cm$^3$ [21]; in Portugal, moisture content between 17 % and 21 % was found, with maximum dry densities between 1.94 g/cm$^3$ and 2.1 g/cm$^3$ [22]; in Canada, moisture content between 14.23 % and 20. 58 %, with maximum dry densities between 1.64 g/cm$^3$ and 1.79 g/cm$^3$ [23]; in Saudi Arabia, moisture contents between 15.55 % and 24.07 % were obtained, with maximum dry densities between 1.60 g/cm$^3$ and 1.76 g/cm$^3$ [24]; and in India, moisture contents between 14.88 % and 25.87 % were reported, with maximum dry densities between 1.60 g/cm$^3$ and 1.78 g/cm$^3$ [25]. In the direct shear test, friction angle (18.77°) and cohesion (5.34 kN/m$^2$) values consistent with other investigations were obtained [26,27].

Table 2 shows the results of compression and flexural tests on compression mold (CM), REW, and REWC samples with a 30-day drying period. The data show a decrease in compressive and flexural strength with the inclusion of natural Arundo donax fiber. These values are similar to the results of other authors; for example, in Bhutan, it was obtained between 0.55 and 1.65 MPa in simple compression [15]; in Portugal, between 0.77 and 1.25 MPa in simple compression and 0.32–0.53 MPa in flexure [14]; in Australia, between 0. 4–0.84 MPa in simple compression [28]; in France, between 0.246 and 0.7 MPa in simple compression and 0.11–0.4 MPa in bending [29]; and in Peru, between 0.25 and 0.58 MPa in simple compression and 0.08–0.2 MPa in bending [30].

Gynerium sagittatum, commonly called the natural fiber of Arundo donax or "caña brava," is used in Colombia to make handicrafts and construct earthen houses. In Santander, Colombia, it is used in the ancestral technique of including natural Arundo donax fiber in building rammed earth walls to improve their strength and flexibility. Despite its long tradition, its effectiveness has not yet been demonstrated. However, previous research on using natural fibers exists, such as [31–37].

The results of the physical and mechanical characterization of the cross and longitudinal sections of Arundo donax reed used in the REWC can be observed in Table 3. The density of the Arundo donax is, on average, 1.28 g/cm3, the tensile strength is 28.84 MPa, and the flexural strength is 0.05 MPa. These results are consistent with research; for example [32], obtained a tensile strength between 168.23 MPa and 59.8 MPa, an elastic modulus between 3.53 and 1.60 GPa, a deformation between 43.17 and 17.7 %, and a density of 1.29 g/cm$^3$ [38].

### *2.2. Manufacture of walls made of rammed earth*

Rammed earth walls need foundations to protect them from humidity and prevent displacement [26,39]. In the past, large rocks, lime, sand, and flat stones were used to create a solid and uniform foundation to support loads and prevent settlement [40]. Today, foundation beams constructed of steel-reinforced concrete are used [41]. A 2.10m × 0.15m x 0.5m steel-reinforced foundation plate and 21 MPa concrete were used (Fig. 2 left), with steel formwork placed on top to construct the walls (Fig. 2 right).

Four walls were constructed for the cyclic test: two walls of compacted soil only as a reference (REW) and two walls with the inclusion of Arundo donax natural fiber (REWC). Approximately 500 kg of CL was used to fabricate each earth wall. The manual process for the REW walls included mixing the material with 20 % water to obtain optimum humidity and compacting it with a hand rammer every 10 cm until a height of 2m was obtained according to the regional technique.

The fabrication of the REWC walls followed the same procedure, compacting layers of 10 cm up to 40 cm. Then, 135 cm and 23 mm diameter longitudinal sections of Arundo donax natural fiber were incorporated, with a separation of 10 cm between them (Fig. 3 left). Subsequently, the compaction process was repeated until a height of 40 cm was achieved, including 35 cm and 25 mm diameter cross sections of Arundo donax natural fiber, separated every 10 cm (Fig. 3 right). This procedure was repeated by interspersing longitudinal and transverse sections until a total height of 2 m was reached. The walls were dried for 30 days, which can affect the strength parameters due to temperature and humidity variation [40]. Once the drying period was over, both sides of the walls were covered with lime, and a grid was drawn to detect deformations during the tests.

### *2.3. Test configuration and instrumentation*

Cyclic lateral load tests were carried out on the stepped slurry walls with a hydraulic actuator positioned at 1.70 m, using a steel

**Table 1**
Physical properties of soils.

| Soil | LL (%) | LP (%) | IP (%) | LC (%) | Fines content (%) | Sand content (%) | Gravel of content (%) |
|---|---|---|---|---|---|---|---|
| **SM** | 39 | 35.67 | 4.13 | 12.5 | 48.92 | 50.46 | 0.62 |
| **CL** | 45.16 | 20.19 | 24.97 | 14.5 | 52.62 | 43.93 | 0.44 |

**Table 2**
Soil mechanical characterization, REW, and REWC.

| Type of sample | Number of samples | Dimensions (cm) | Compressive stress (MPa) | Young's module E (MPa) | Shear stress Cu (MPa) | Tensile stress (MPa) |
|---|---|---|---|---|---|---|
| **CM** | 10 | 30 x 15 | 0.31 | 63.64 | 0.155 | 0.105 |
| **REW** | 2 | 900 x 200 x 1000 | 0.64 | 117.33 | 0.32 | – |
| **REWC** | 2 | 900 x 200 x 1000 | 0.48 | 64.76 | 0.24 | – |

**Table 3**
Physical and mechanical characterization of Arundo donax.

| Type of sample | Number of samples | Diameter (cm) | Tensile stress (MPa) | Traction stress (MPa) | Density (g/cm$^3$) |
|---|---|---|---|---|---|
| Longitudinal sections of 135 cm of Arundo donax | 5 | 22.68 | 0.04 | 24.39 | 1.33 |
| Transverse sections of 35 cm of Arundo donax | 5 | 25.66 | 0.06 | 33.3 | 1.23 |


**Fig. 2.** Left: foundation and right: formwork.

**Fig. 3.** Arundo donax left: Longitudinal sections and right: transversal sections.

frame hinged at all joints (Fig. 4 left). This frame was mainly used to avoid local failures in the interaction between the wall and the hydraulic actuator, as well as to evaluate the actual behavior of the REW [18].

The applied compressive load was 13 kPa at the top of the wall, simulating the vertical load generated by the roof of a rammed-earth house, like how it was performed [40]. This load was applied by concrete beams with the help of a crane. Other authors applied higher loads to the wall to restrain movement and prevent rocking. Among them, Miccoli et al., applied compressive stress of 0.56 N/mm2 [42], Romanazzi et al., of 0.3 MPa [22] and Wangmo et al., of 0.1 MPa to their L-shaped wall [15]. However, the purpose of the research was not to evaluate the shear strength of the walls but to evaluate the failure modes against seismic loads, so it was considered pertinent first not to restrict the movement and second to apply an actual load generated by the roof of a house.

Finally, two LDVT (Linear Differential Displacement Transformer) transducers were installed on a concrete column to measure the

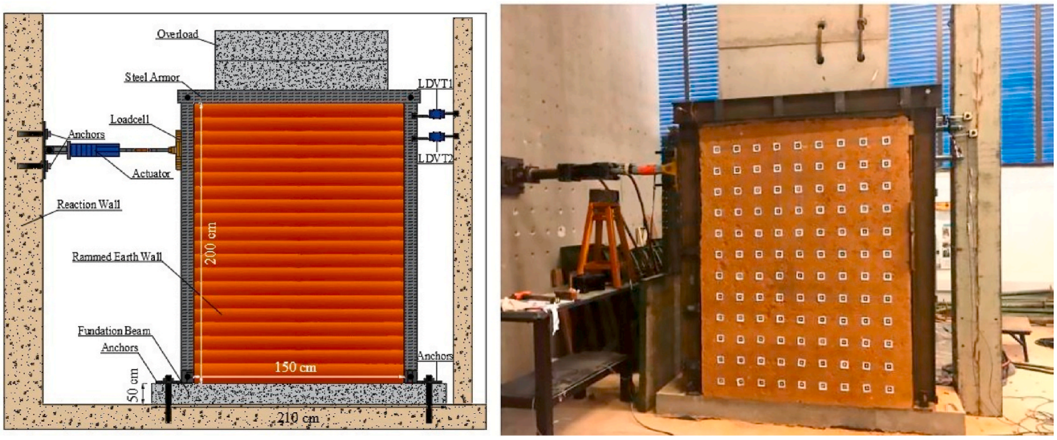


**Fig. 4.** Left: Equipment configuration and right: Cyclic test.

wall displacement during cyclic load tests. Due to equipment limitations, the movement was limited to a maximum drift of 1.4 % of the total wall height. The cyclic horizontal push and pull loads are exerted by a hydraulic actuator connected to a reaction wall at the top. The displacement control of the cyclic lateral load test was performed visually through the monitor of the hydraulic unit until the maximum drift was reached (Fig. 4 left).

Similar instrumentation has been used in previous investigations to evaluate the strength of walls made of various materials, including polypropylene fibers [7], steel plates [9], steel rods, steel mesh [26], wood [38], glass fibers [15], cement, lime, or fly ash [27].

In the push and pull test, horizontal cyclic displacements of increasing amplitude of 3.8 mm were applied for each step, corresponding to a drift of 0.2 %, repeated three times for each displacement amplitude until a drift of 1.4 % was reached (Fig. 4 right). This value was calculated considering the limited displacement range of (3.8 mm–22.6 mm).

## 3. Results and discussion

The walls were subjected to the inverse cyclic displacement protocol, based on FEMA 461 [43] it is shown in Fig. 5. This protocol started with cycles of 3.8 mm amplitude (equivalent to 0.2 % drift), which were subsequently increased by the same amount until failure was reached with a drift of 1.4 % for REW walls and 1 % for REWC walls. Consistent with the methodology used by Ramezanpour et al., in his research [27] Three complete displacement cycles were used to evaluate each configuration of the push-pull force relationship.

Fig. 6 represents the maximum push and pull loads, which differ because of damage in reverse loading cycles, agreeing with Miccoli's results [44]. In the push test, resistance to movement must be overcome, while in the pull, the weight of the wall acts as an additional force requiring less force, in line with Vatani's findings [37]. Rammed earth walls showed varying strength and deformation capacities under cyclic thrust and tensile loads. REW tended to have higher load-bearing capacities in both thrust and tension compared to REWC. This suggests that the inclusion of natural fibers in horizontal positions may significantly affect the strength and behavior of the wall under cyclic loading due to differences in the tensile strength and ductility of the material.

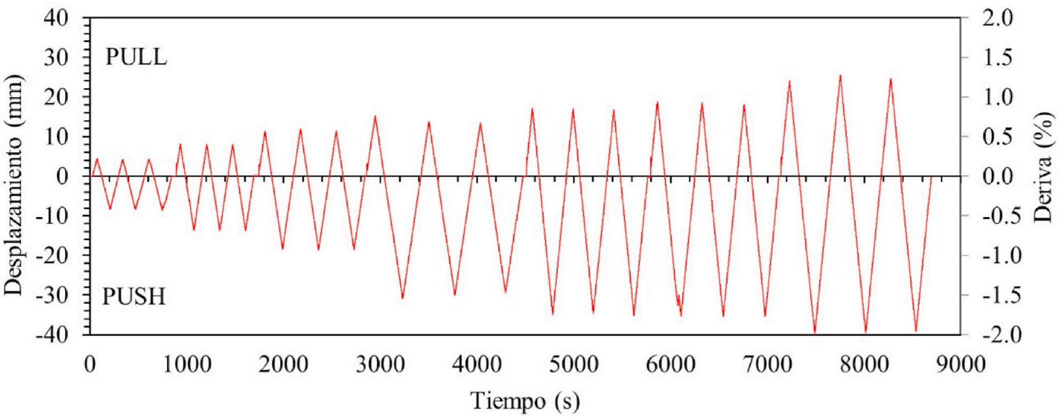


**Fig. 5.** Reverse cyclic loading protocol.

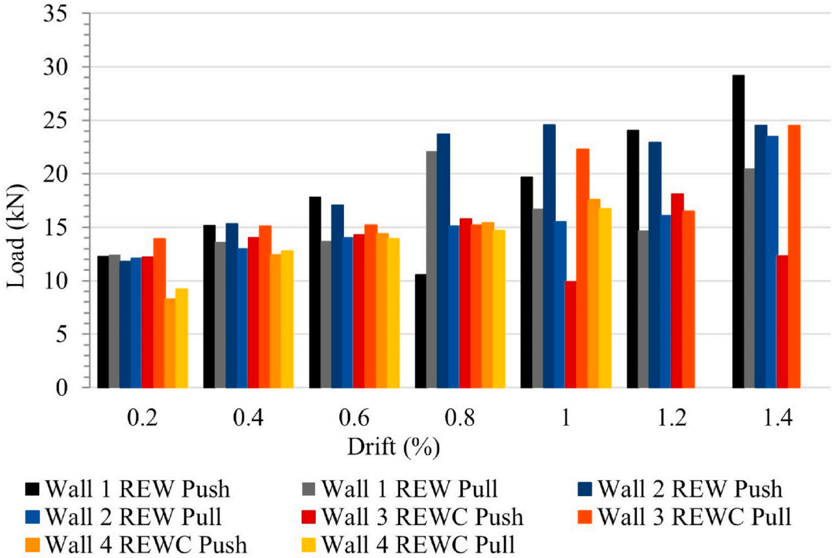


**Fig. 6.** Maximum push and pull loads vs drifts.

During cyclic loading, the relationship between maximum displacement and force was monitored in real-time to obtain the hysteretic responses of all walls. The horizontal load hysteresis loops and the corresponding displacement obtained from the cyclic curves for each load step are shown in Fig. 7. According to Miccoli et al. [44], the shape of the hysteresis loops is typical of shear failure due to limited sliding of the rammed earth layers, where the occurrence of cracks was presented at a drift of 0.69 % and the maximum drift

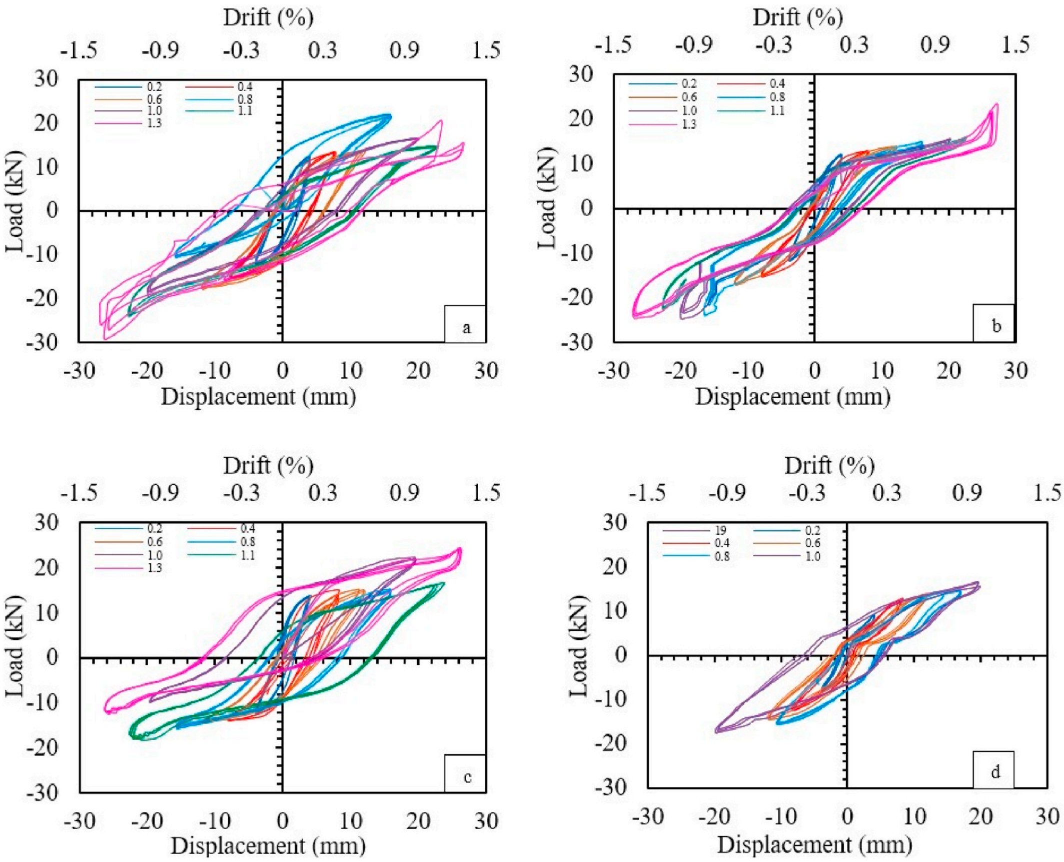


**Fig. 7.** Cyclic load-displacement curve; a) RWE 1, b) REW 2, c) REW 3 and d) REW 4.

reached was 1.47 %. The load and displacement capacities for REW 1 are 29.2 kN - 26.88 mm (push) and 20.5 kN - 26.64 mm (pull) (Fig. 7-a). Wall REW 2 recorded in Fig. 7-b load capacities of 24.5 kN with a maximum push displacement of 27.14 mm and 23.5 kN with a maximum pull displacement of 27.23 mm.

Walls REWC 3 and REWC 4 reached a drift of 0.8 and 1 %, respectively, producing a localized shear failure in the first Arundo donax natural fiber inclusion. In wall REWC 3, the maximum push load was 12.3 kN with a displacement of 26.28 mm, and the maximum pull load was 24.5 kN with a displacement of 26.45 mm (Fig. 7-c). In wall REWC 4, the load capacities of 17.6 kN (push) with a displacement of 19.92 mm and 16.7 kN (pull) with a displacement of 19.86 mm were recorded (Fig. 7-d). The resistance of the walls to cyclic loads is attributed to the mechanical properties of the component materials, such as compressive strength, flexural strength, cohesion, friction, and elastic modulus.

As the loading cycle progresses, the hysteretic curves initially show a brief period of linear elasticity that widens with increasing drift. According to Zhou et al. [45], this widening of the loops is due to the dissipation of microcosmic cracks induced by the energy applied during horizontal cyclic loading. The hysteresis envelope curves are based on the first cycle of each displacement amplitude, reflecting a consistency like that observed in the results of Miccoli et al., [44]. Arslan et al. [46], suggests that this behavior indicates the presence of plastic deformations and energy dissipation in the form of heat, attributable to friction and internal deformation of the material. In the REWC, a significant reduction in strength was observed under cyclic loading. Hysteresis loops showed a typical shear failure, indicating limited sliding between the rammed earth layers where the natural fibers were included and a lower capacity to resist deformations. Compared to the REW, the REWCs exhibited markedly lower load-bearing capacities, underlining the crucial influence of the material's mechanical properties on their structural behavior under dynamic conditions.

Fig. 8 represents the lateral load-displacement envelope of the walls; these curves were obtained by connecting the maximum points of the first cycles of the loading history in both directions. As stated by Romanazzi et al. [14], although there is asymmetry in the hysteresis curves, the analysis exclusively centers on the maximum horizontal loads in the force quadrant and horizontal displacements, thereby streamlining the evaluation of structural capacity under lateral loads. To investigate the effect of including Arundo donax natural fiber on the lateral load capacity, two specimens should be compared with their REW counterpart. All walls behaved similarly, moving as rigid bodies with drifts between 0.2 % and 1.4 %. Ramezanpour et al. [47], notes that typically, the failure modes observed during the can be classified as rocking and shear [27]. In the study, it was observed that REWs walls did not reach failure. However, REWC wall 3 was found to fail with a 1 % drift, supporting a load of 22.3 kN, while REWC wall 4 failed with a drift of 0.8 % under a load of 17.6 kN. This could be the result of a lower cohesion between the compacted soil layers and the fibers. This lower cohesion facilitates sliding and crack formation under cyclic loading. In addition, it has been suggested that the asymmetry in the hysteresis curves could be attributed to different behaviors in the thrust and tensile directions. Miccoli et al. [44], points out that this phenomenon is frequent in walls built with heterogeneous materials such as rammed earth.

One measure of a structure's resistance to seismic loading is its ability to dissipate seismic energy. As noted by Ramezanpour et al. [27], and Sakr et al. [48], in cyclic loading, dissipated energy is defined as the energy lost during each hysteretic cycle. The dissipation energy is specified as the area under the force-displacement hysteresis envelope curve [48]. The total energy dissipation capacity ($E_{td}$) is calculated by summing the energy absorbed during each load cycle ($E_{di}$), as seen in Equation (1).

$$E_{td} = \sum_{i}^{n} E_{di} \tag{1}$$

Fig. 9 shows the variation of the total dissipated energy as a function of lateral drift for the tested walls. REW wall 1 reached the

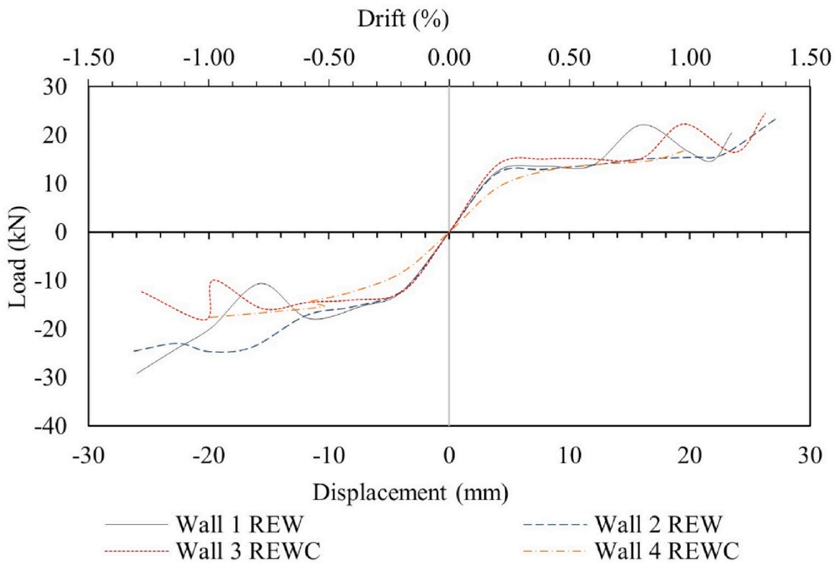


**Fig. 8.** Load-displacement envelope curves of test walls.

accumulated dissipated energy of 5008.11 kNmm, while REW wall 2 reached 3593.49 kNmm. On the other hand, wall 3 and wall 4 experienced a notable reduction in dissipated energy, with values of 2477.57 kNmm and 1845.68 kNmm, respectively. This shows that unreinforced rammed earth walls absorb and dissipate more energy during load cycles, improving seismic resistance, while the inclusion of Arundo donax fibers reduced the energy dissipation capacity having an adverse effect.

Arslan et al. [46], describes the use of stiffness degradation to the overall response of the test specimens. Stiffness is calculated through the slope of the load-deflection curve joining the positive and negative peaks obtained during the tests using equation (2)

$$K_i = \frac{F_i^+ - F_i^-}{D_i^+ - D_i^-} \tag{2}$$

Where $F_i^+$ y $F_i^-$ are the maximum loads corresponding to displacements $D_i^+$ y $D_i^-$ in the push and pull directions.

Fig. 10 shows a steady decrease in the stiffness of all walls as the drift ratio increases, this loss of stiffness is due to cumulative damage caused by drift in each cycle. REW 1, REW 2 and REWC 3 achieved similar maximum stiffness values of 3.9 kN/mm, 3.07 kN/mm and 3.38 kN/mm, respectively. But the maximum stiffness of REWC 4 was notably lower, with a value of 2.1 kN/mm. According to Tripura et al. [49], in structures such as rammed earth walls, where strength and stiffness are key against lateral forces, horizontal fibers do not effectively reinforce in the critical direction. Stiffness depends on the fibers to resist vertical or oblique forces, where vertical fibers may offer better reinforcement.

The test walls presented a rigid behavior evidenced in Fig. 10 by their failure pattern. This behavior is due to the mechanical properties of the materials, such as tensile strength, compressive strength, and elastic modulus. REW 1 and REW 2 swayed during the test and showed cracks at the tip, but did not fail, behaving as a rigid body (Fig. 11). The unreinforced rammed earth wall showed a relatively greater capacity to resist deformations without fracturing, evidencing its inherent structural robustness.

REWC 3 and REWC 4 swayed and presented horizontal cracks, which generated a failure surface with a drift of 0.8 %. The failure mode identified was shear in the first layer of Arundo donax natural fiber inclusion 40 cm from the foot of the wall. The intercalation of these natural fibers created a plane of weakness that experienced progressive shear at each drift cycle, culminating in failure, as shown in Fig. 12.

Currently, there is little documentation on the use of Arundo donax, cane, bamboo or other similar materials as reinforcement in rammed earth walls. Variations are significant depending on the country and technique used. For example, in Peru, the 2017 standard E.080 specifies the use of Arundo donax (diameter 25 mm) in adobe constructions with horizontal reinforcements every 40 cm transversely, every 18 cm longitudinally and every 35 cm vertically [50]. On the other hand, in India, the IS13837:1993 standard mentions horizontal and vertical reinforcements, suggesting the use of bamboo mesh without specifying dimensions [51]. Finally, in Colombia, the only section of the seismic resistant standard called AIS 610-EP-17 focuses on heritage buildings with wood, steel or plastic reinforcements, excluding reed reinforcements and not applying to new constructions [52].

Standards such as NBC 204:1994 [53], NZS 4297:1998 [54] and ASTM E2392-M10:2010 [55] recommend horizontal reinforcement with concrete or steel to resist seismic forces, although in rural areas the use of bamboo or wood may be necessary due to cost and supply constraints. However, it is cautioned that horizontal reinforcing bars could weaken the structure and cause cracks, affecting the shear strength of the walls [56]. In contrast, vertical reinforcement, which is more common, uses steel and concrete to protect structural integrity and prevent separation between the walls and the foundation from seismic forces.

The analysis revealed that the technique of incorporating Arundo donax in the horizontal layer in the region of Santander, Colombia, generates failure planes that affect the structural resistance of the wall against cyclic loads. As an improvement, it is suggested to study the vertical inclusion of Arundo donax or to combine vertical steel reinforcement with Arundo donax in the horizontal layer. These options could redistribute the internal forces of the wall and strengthen its capacity to resist and dissipate energy under dynamic loads. Tripura et al. [12], investigated a similar case with treaded rammed earth walls, using bamboo for horizontal reinforcement and steel for vertical reinforcement, demonstrating its effectiveness in low-rise constructions.

## 4. Conclusions

This study carried out research on ancestral technique of rammed earth walls with inclusion of Arundo donax fiber performed in Santander, Colombia. The soil material used in the construction of rammed earth walls is essential to provide physical, mechanical and durability properties to the structure. A suitable proportion between 20 % and 40 % clay and between 60 % and 80 % sand in the mix is recommended. Clay provides cohesion and plasticity to the mix, while sand provides strength and stability. Insufficient clay affects the quality and durability of the wall, while too much clay produces a sticky, difficult-to-work mixture. Sand alone prevents the formation of a strong, durable structure. The combination of clay and sand in a homogeneous mixture allows for a solid and resistant structure with ideal compaction and malleability.

REW 2 presented a higher moisture content than the optimum established by the moisture-density ratio test, which explains the variability of the results between REW 1 and REW 2. It is essential to achieve the optimum moisture content by means of the Proctor test in the construction of masonry walls, since this has a direct impact on the strength and durability of the wall. Too much dryness or humidity can lead to deformation, collapse or cracking.

The instrumentation and the base of the walls performed optimally, thanks to the articulated frame that allowed movement under cyclic loads without causing local failures due to the hydraulic actuator. Despite limitations in displacement measurement, the LDVT transducers demonstrated accuracy, providing reliable data on the structural behavior of the walls.

The REWC walls demonstrated lower load carrying capacity under cyclic loads according to the FEMA 461 protocol compared to

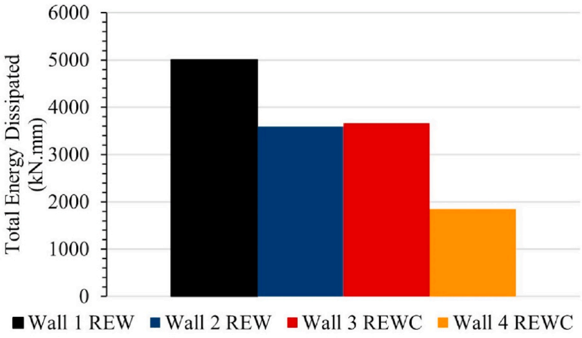


**Fig. 9.** Energy dissipated in the test walls under cyclic loading.

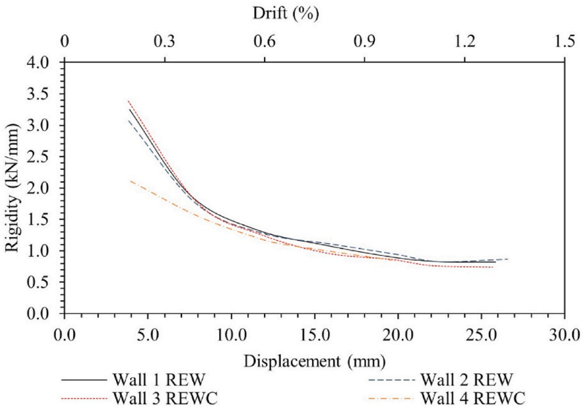


**Fig. 10.** Wall stiffness degradation curves.

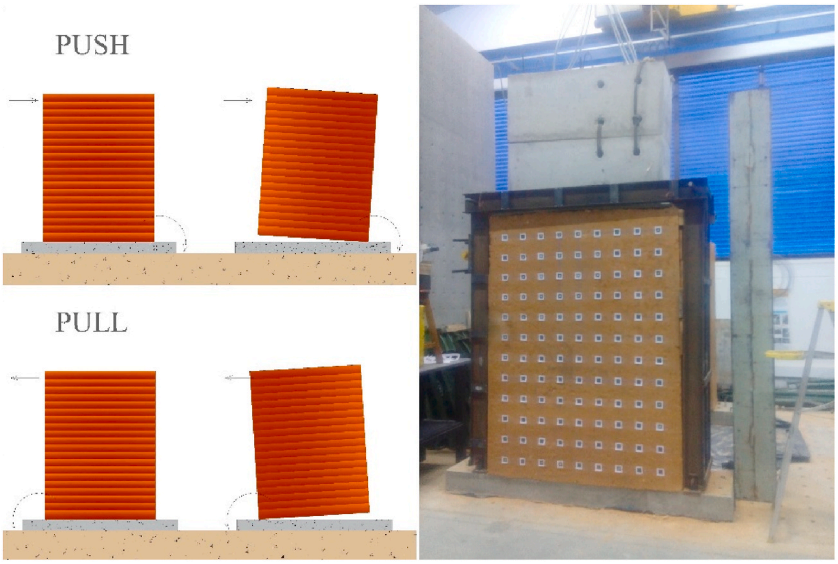


**Fig. 11.** Failure pattern REW Rigid body.

the REW walls. REWC walls achieved 12.3 kN and 24.5 kN in thrust and tension, respectively, while REW walls showed higher capacities of 29.2 kN and 20.5 kN under the same loading conditions.

The results of the study show that there is a difference between the maximum cyclic push and pull loads, which is because of the


**Fig. 12.** REWC failure pattern failure plane.

damage that occurs during the reverse loading cycles. The difference is that in the push test the resistance to movement must be overcome, whereas in the pull test the weight of the wall adds additional force, which requires less effort.

The hysteresis plots show that REW 1 and REW 2 have a better capacity to resist lateral cyclic loads than REWC 3 and REWC 4. This is because the latter have longitudinal and cross sections that weaken the wall, creating a progressive plane of weakness in thrust and backward movements. All the walls have a similar behavior for a drift between 0.2 % and 0.8 % in terms of load capacity and dissipated energy. However, REWC 3 and REWC 4 failed with a drift of 0.8 % and 1 %, respectively, causing the division of the wall into two independent sections that behave as rigid bodies, where the upper section slides and rotates due to the load exerted.

During the cyclic displacement tests, it was observed that the REWC walls showed a typical form of shear failure, evidencing a less robust performance in strength and deformation capacity compared to the REW walls. This is attributed to the inclusion of Arundo donax fibers, which introduce planes of weakness and affect the cohesion between the rammed earth layers, facilitating crack formation and slippage under dynamic loads.

The energy dissipation plots provide information on which element behaves more rigidly by showing which element required more work to be displaced. REW 1 and REW 2 had the highest cumulative dissipated energy, while REWC 3 and REWC 4 experienced a noticeable reduction in dissipated energy by reaching drifts of 0.8 % and 1 %, respectively, prior to failure. REW walls demonstrated a greater capacity to absorb and dissipate energy during load cycling, with significantly higher cumulative dissipated energy values compared to REWC walls. This highlights the importance of evaluating the impact of natural fiber inclusion on the seismic response and structural safety of rammed earth walls.

The structural stiffness of all walls gradually decreased with increasing lateral drift, due to cumulative damage during loading cycles. The REWC walls, especially REWC 4, exhibited noticeably lower maximum stiffness compared to the REW walls, suggesting a less effective structural response to lateral loads.

The inclusion of natural fibers such as Arundo donax in rammed earth walls should be optimized to mitigate adverse effects on structural strength and seismic load bearing capacity. The use of this construction method is not appropriate for the study region, and the lack of regulations in new earth construction carries risks. It is recommended to investigate strategies that include Arundo donax vertically or combined with vertical reinforcement to improve strength and seismic response.

## Statement

During the preparation of this work, the authors used "ChatGPT Openai" to improve the writing process. After using this tool, the authors reviewed and edited the content as needed and took full responsibility for the publication's content.

## Data availability statement

Data associated with the study are not in a publicly available repository. Data will be available upon request.

## CRediT authorship contribution statement

**Viviana Mora-Ruiz:** Writing – review & editing, Methodology, Investigation, Formal analysis, Data curation, Conceptualization. **Cristian Mejía-Parada:** Validation, Supervision, Methodology, Investigation, Formal analysis, Data curation, Conceptualization.

**Brayam Nuñez:** Writing – review & editing, Supervision, Investigation, Data curation. **Sergio Pineda:** Writing – review & editing, Supervision, Conceptualization. **Néstor I. Prado:** Writing – review & editing, Conceptualization. **Jose Agustin Vallejo-Borda:** Writing – review & editing, Conceptualization. **Jair Arrieta-Baldovino:** Writing – review & editing.

## Declaration of competing interest

The authors declare that they have no known competing financial interests or personal relationships that could have appeared to influence the work reported in this paper.

## Acknowledgements

We are grateful to the research and development university for their valuable collaboration during the execution of the manuscript. In addition, we would like to express our gratitude to the Pontifical Bolivarian University, especially the materials laboratory, for facilitating the use of their facilities during the experimental phase. These collaborations were fundamental to carrying out our study and contributed significantly to the results obtained.

## References

[1] A. Chel, G. Kaushik, Renewable energy technologies for sustainable development of energy efficient building, Alex. Eng. J. 57 (2018) 655–669, https://doi.org/10.1016/j.aej.2017.02.027.
[2] P.A. Jaquin, C.E. Augarde, C.M. Gerrard, Chronological description of the spatial development of rammed Earth techniques, Int. J. Architect. Herit. 2 (2008) 377–400, https://doi.org/10.1080/15583050801958826.
[3] D. Ciancio, P. Jaquin, P. Walker, Advances on the assessment of soil suitability for rammed earth, Constr Build Mater 42 (2013) 40–47, https://doi.org/10.1016/j.conbuildmat.2012.12.049.
[4] D. Arduin, L.R. Caldas, R. de L.M. Paiva, F. Rocha, Life cycle assessment (lca) in earth construction: a systematic literature review considering five construction techniques, Sustainability 14 (2022), https://doi.org/10.3390/su142013228.
[5] T. Zhou, Z. Zhang, Z. Su, P. Tian, Seismic performance test of rammed earth wall with different structural columns, Adv. Struct. Eng. 24 (2021) 107–118, https://doi.org/10.1177/1369433220944506.
[6] H. Araki, J. Koseki, T. Sato, Tensile strength of compacted rammed earth materials, Soils Found. 56 (2016) 189–204, https://doi.org/10.1016/j.sandf.2016.02.003.
[7] A. Karrech, V. Strazzeri, M. Elchalakani, Improved thermal insulance of cement stabilised rammed earth embedding lightweight aggregates, Constr Build Mater 268 (2021), https://doi.org/10.1016/j.conbuildmat.2020.121075.
[8] A.H. Meek, M. Elchalakani, C.T.S. Beckett, M. Dong, Alternative stabilised rammed earth materials incorporating recycled waste and industrial by-products: a study of mechanical properties, flexure and bond strength, Constr Build Mater 277 (2021), https://doi.org/10.1016/j.conbuildmat.2021.122303.
[9] A. Romanazzi, D.V. Oliveira, R.A. Silva, Experimental investigation on the bond behavior of a compatible TRM-based solution for rammed earth heritage, Int. J. Architect. Herit. 13 (2019) 1042–1060, https://doi.org/10.1080/15583058.2019.1619881.
[10] M. Fagone, F. Loccarini, G. Ranocchiai, Strength evaluation of jute fabric for the reinforcement of rammed earth structures, Compos. B Eng. 113 (2017) 1–13, https://doi.org/10.1016/j.compositesb.2016.12.054.
[11] A.E. Losini, A.C. Grillet, L. Vo, G. Dotelli, M. Woloszyn, Biopolymers impact on hygrothermal properties of rammed earth: from material to building scale, Build. Environ. 233 (2023), https://doi.org/10.1016/j.buildenv.2023.110087.
[12] D.D. Tripura, K.D. Singh, Mechanical behaviour of rammed earth column: a comparison between unreinforced, steel and bamboo reinforced columns, Mater. Construcción 68 (2018), https://doi.org/10.3989/mc.2018.11517.
[13] B. Sen, R. Saha, Experimental and numerical investigation of mechanical strength characteristics of natural fiber retrofitted rammed earth walls, Geotext. Geomembranes 50 (2022) 970–993, https://doi.org/10.1016/j.geotexmem.2022.06.004.
[14] A. Romanazzi, D.V. Oliveira, R.A. Silva, A. Barontini, N. Mendes, Performance of rammed earth subjected to in-plane cyclic displacement, Materials and Structures/Materiaux et Constructions 55 (2022), https://doi.org/10.1617/s11527-022-01894-z.
[15] P. Wangmo, K.C. Shrestha, T. Aoki, Exploratory study of rammed earth walls under static element test, Constr Build Mater 266 (2021), https://doi.org/10.1016/j.conbuildmat.2020.121035.
[16] T.L. Bui, T.T. Bui, Q.B. Bui, X.H. Nguyen, A. Limam, Out-of-plane behavior of rammed earth walls under seismic loading: finite element simulation, Structures 24 (2020) 191–208, https://doi.org/10.1016/j.istruc.2020.01.009.
[17] A. Perić, I. Kraus, J. Kaluđer, L. Kraus, Experimental campaigns on mechanical properties and seismic performance of unstabilized rammed earth—a Literature Review, Buildings 11 (2021), https://doi.org/10.3390/buildings11080367.
[18] M.E. Arslan, M. Emiroğlu, A. Yalama, Structural behavior of rammed earth walls under lateral cyclic loading: a comparative experimental study, Constr Build Mater 133 (2017) 433–442, https://doi.org/10.1016/j.conbuildmat.2016.12.093.
[19] V. Maniatidis, P. Walker, Structural capacity of rammed earth in compression, J. Mater. Civ. Eng. 20 (2008) 230–238.
[20] M. Emiroğlu, A. Yalama, Y. Erdoğdu, Performance of ready-mixed clay plasters produced with different clay/sand ratios, Appl. Clay Sci. 115 (2015) 221–229, https://doi.org/10.1016/j.clay.2015.08.005.
[21] P. Zare, S. Sheikhi Narani, M. Abbaspour, A. Fahimifar, S.M. Mir Mohammad Hosseini, P. Zare, Experimental investigation of non-stabilized and cement-stabilized rammed earth reinforcement by Waste Tire Textile Fibers (WTTFs), Constr Build Mater 260 (2020), https://doi.org/10.1016/j.conbuildmat.2020.120432.
[22] R. Ramírez Eudave, R.A. Silva, E. Pereira, A. Romanazzi, Early-age shrinkage and bond of LC-TRM strengthening in rammed earth, Constr Build Mater 350 (2022), https://doi.org/10.1016/j.conbuildmat.2022.128809.
[23] S.S. Narani, P. Zare, M. Abbaspour, A. Fahimifar, S. Siddiqua, S.M. Mir Mohammad Hosseini, Evaluation of fiber-reinforced and cement-stabilized rammed-earth composite under cyclic loading, Constr Build Mater 296 (2021), https://doi.org/10.1016/j.conbuildmat.2021.123746.
[24] Y.M.H. Mustafa, M.S. Zami, O.S.B. Al-Amoudi, M.A. Al-Osta, Y.S. Wudil, Analysis of unconfined compressive strength of rammed earth mixes based on artificial neural network and statistical analysis, Materials 15 (2022), https://doi.org/10.3390/ma15249029.
[25] S.S.D. Raavi, D.D. Tripura, Evaluating the flexural strength and failure patterns of cement stabilized rammed earth wallettes reinforced with coir, bamboo and steel, Materials and Structures/Materiaux et Constructions 55 (2022), https://doi.org/10.1617/s11527-022-01896-x.
[26] D.M. Ruiz, J.C. Reyes, C. Bran, M. Restrepo, Y.A. Alvarado, N. Barrera, C. Laverde, D. Suesca, Flexural behavior of rammed earth components reinforced with steel plates based on experimental, numerical, and analytical modeling, Constr Build Mater 320 (2022), https://doi.org/10.1016/j.conbuildmat.2021.126231.
[27] M. Ramezanpour, A. Eslami, H. Ronagh, Seismic performance of stabilised/unstabilised rammed earth walls, Eng. Struct. 245 (2021), https://doi.org/10.1016/j.engstruct.2021.112982.
[28] D. Ciancio, C.T.S. Beckett, J.A.H. Carraro, Optimum lime content identification for lime-stabilised rammed earth, Constr Build Mater 53 (2014) 59–65, https://doi.org/10.1016/j.conbuildmat.2013.11.077.

[29] E. Araldi, E. Vincens, A. Fabbri, J.P. Plassiard, Identification of the mechanical behaviour of rammed earth including water content influence, Materials and Structures/Materiaux et Constructions 51. https://doi.org/10.1617/s11527-018-1203-2, 2018.
[30] M.I. Gomes, T.D. Gonçalves, P. Faria, Unstabilized rammed earth: characterization of material collected from old constructions in south Portugal and comparison to normative requirements, Int. J. Architect. Herit. 8 (2014) 185–212, https://doi.org/10.1080/15583058.2012.683133.
[31] A. Laborel-Préneron, C. Magniont, J.E. Aubert, Hygrothermal properties of unfired earth bricks: effect of barley straw, hemp shiv and corn cob addition, Energy Build. 178 (2018) 265–278, https://doi.org/10.1016/j.enbuild.2018.08.021.
[32] M. Giroudon, A. Laborel-Préneron, J.E. Aubert, C. Magniont, Comparison of barley and lavender straws as bioaggregates in earth bricks, Constr Build Mater 202 (2019) 254–265, https://doi.org/10.1016/j.conbuildmat.2018.12.126.
[33] H. Danso, D.B. Martinson, M. Ali, J.B. Williams, Physical, mechanical and durability properties of soil building blocks reinforced with natural fibres, Constr Build Mater 101 (2015) 797–809, https://doi.org/10.1016/j.conbuildmat.2015.10.069.
[34] P. Nshimiyimana, D. Miraucourt, A. Messan, L. Courard, Calcium carbide residue and rice husk ash for improving the compressive strength of compressed earth blocks, MRS Adv 3 (2018) 2009–2014, https://doi.org/10.1557/adv.2018.147.
[35] M.C.N. Villamizar, V.S. Araque, C.A.R. Reyes, R.S. Silva, Effect of the addition of coal-ash and cassava peels on the engineering properties of compressed earth blocks, Constr Build Mater 36 (2012) 276–286, https://doi.org/10.1016/j.conbuildmat.2012.04.056.
[36] A.W. Bruno, D. Gallipoli, C. Perlot, H. Kallel, Thermal performance of fired and unfired earth bricks walls, J. Build. Eng. 28 (2020), https://doi.org/10.1016/j.jobe.2019.101017.
[37] A. Vatani Oskouei, M. Afzali, M. Madadipour, Experimental investigation on mud bricks reinforced with natural additives under compressive and tensile tests, Constr Build Mater 142 (2017) 137–147, https://doi.org/10.1016/j.conbuildmat.2017.03.065.
[38] C. Tenorio, R. Moya, M.T. Filho, J. Valaert, Quality of pellets made from agricultural and forestry crops in costa rican tropical climates, Bioresources 10 (2015) 482–498, https://doi.org/10.15376/biores.10.1.482-498.
[39] J.C. Reyes, L.E. Yamin, W.M. Hassan, J.D. Sandoval, C.D. Gonzalez, F.A. Galvis, Shear behavior of adobe and rammed earth walls of heritage structures, Eng. Struct. 174 (2018) 526–537, https://doi.org/10.1016/j.engstruct.2018.07.061.
[40] A. Fabbri, J.-C. Morel, J.-E. Aubert, Q.-B. Bui, D. Gallipoli, V. Reddy, Testing and Characterisation of Earth-Based Building Materials and Elements, Springer, Springer International Publishing, Cham, 2022, https://doi.org/10.1007/978-3-030-83297-1.
[41] J.C. Morel, E. Toussaint, C. Auvergne, A. Fabbri, Y. Sieffert, O. Ple, Mechanical Behavior of Rammed Earth Walls under Pushover Tests, Communauté Université Grenoble Alpes, 2017.
[42] L. Miccoli, A. Drougkas, U. Müller, In-plane behaviour of rammed earth under cyclic loading: experimental testing and finite element modelling, Eng. Struct. 125 (2016) 144–152, https://doi.org/10.1016/j.engstruct.2016.07.010.
[43] FEMA 461, Interim Testing Protocols for Determining the Seismic Performance Characteristics of Structural and Nonstructural Components, 2007. Washington, D.C. www.ATCouncil.org.
[44] L. Miccoli, P. Fontana, U. Müller, P. Fontana, Strengthening of rammed earth structural elements. Mechanical behaviour under shear and cyclic loading, in: COMPDYN 2017 - Proceedings of the 3th International Conference on Protetionn of Historical Constructions, National Technical University of Athens, Germany, 2017, pp. 1–9. https://www.researchgate.net/publication/318469404.
[45] T. Zhou, B. Liu, X. Zhao, J. Mu, Experimental testing of the in-plane behavior of bearing modern rammed earth walls, Adv. Struct. Eng. 21 (2018) 2045–2055, https://doi.org/10.1177/1369433218764978.
[46] M.E. Arslan, A. Durmuş, M. Hüsem, Cyclic behavior of GFRP strengthened infilled RC frames with low and normal strength concrete, Sci. Eng. Compos. Mater. 26 (2019) 30–42, https://doi.org/10.1515/secm-2017-0060.
[47] M. Ramezanpour, A. Eslami, H. Ronagh, Seismic performance of stabilised/unstabilised rammed earth walls, Eng. Struct. 245 (2021), https://doi.org/10.1016/j.engstruct.2021.112982.
[48] M.A. Sakr, S.R. El-Khoriby, A.A. Seleemah, M.M. Aboelnour, B. Osama, Experimental and numerical investigation on cyclic behavior of masonry infilled RC frames retrofitted with partially bonded CFRP strips, Structures 33 (2021) 2238–2252, https://doi.org/10.1016/j.istruc.2021.05.087.
[49] D.D. Tripura, K.D. Singh, Axial load-capacity of bamboo-steel reinforced cement stabilised rammed earth columns, Struct. Eng. Int. 29 (2019) 133–143, https://doi.org/10.1080/10168664.2019.1528705.
[50] E.080, Diseño y construcción con tierra reforzada, Perú, 2017. www.construccion.org.
[51] Indian Standard, IS 13837, Improving Earthquake Resistance of Earthen Buildings – Guidelines, Vol. 1993 (1993) 1–14.
[52] AIS 610-EP-17, Evaluación e intervención de edificaciones patrimoniales de uno y dos pisos de adobe y tapia pisada. www.mincultura.gov.co, 2017.
[53] NBC 204:1994, Guidelines for Earthquake Resistant Building Construction: Earthen Building, 2015. Nepal.
[54] NZS 4297:1998, Engineering design of earthen buildings, Vol. 1998 (1998) 1–63.
[55] ASTM E 2392-M10, Standard guide for design of earthen wall building systems, Vol 4 (2010) 1–10.
[56] L. Miccoli, U. Müller, S. Pospíšil, Rammed earth walls strengthened with polyester fabric strips: experimental analysis under in-plane cyclic loading, Constr Build Mater 149 (2017) 29–36, https://doi.org/10.1016/j.conbuildmat.2017.05.115.